

The Kalman Filter in Power Quality – Theory and Applications

Mario González and Víctor Cárdenas
University of San Luis Potosí, UASLP
Mexico

1. Introduction

Power quality is a topic in the area of engineering that emerged by the 1970 decade. It is a field that has attracted special interest recently due to the continuous industrial growth, to the raise of power demands, and to the proliferation of “polluting” electrical loads. One of the objectives of power quality is to meet a clean sinusoidal, stable, reliable, regulated, and uninterrupted supply voltage in electrical systems, in order to feed the so-called *critical loads*. A critical load is such an equipment that, if it fails or works inadequately, it can cause very high losses, being economical, or of any class; and a low quality supply can cause this situation. For example, it can cause the loss of vital information, interruption of an expensive industrial process, poor quality or damage to products; interruption of important communications as air traffic control, security units, and financial information; permanent damage to equipments, and even put lives in danger at hospitals.

The great increment in critical processes has led to the requirement of assuring a high quality and safe power supply in many medical, communications, and industrial procedures, with the aim of feeding machinery and automatic systems that perform diverse important tasks. A safe protection of the operations is the objective.

Problems and failures in electrical loads can be caused by some of the disturbances that exist in electrical systems. Among them are: *harmonic distortion, unbalances, non characteristic harmonics, sags, swells, short and long interruptions, flicker, and short circuits*. The disturbances that more affect critical loads, specially the industrial kind, are the sags, the swells, and the interruptions. The sag is defined as a 10% to 90% decrement of the nominal value of voltage, which can last from a half cycle to one minute. The swell is defined in a similar way, but represented by the 10% to 80% increase of the nominal value (IEEE Std 1159-1995, 1995), (IEEE Std 1159.3-2003, 2004).

Sags have been identified as the most severe disturbance, and as the one that more causes damages and problems to facilities and equipments. It is considered that sags, together with momentary interruptions, are responsible of the 92% of power quality problems that face typical industrial consumers (Bhadkamkar et al., 2003). Sags can be caused by atmospheric discharges, short circuits, energizing of motors and high power loads, operation of soldering machines, and arc furnaces, to mention some. The swells can be caused by disconnections of high power loads from the grid. As can be noted, the disturbances can be generated by natural cause, by neighbor installations, or by accident. It is always desirable their

Source: Kalman Filter, Book edited by: Vedran Kordić,
ISBN 978-953-307-094-0, pp. 390, May 2010, INTECH, Croatia, downloaded from SCIYO.COM

elimination at the origin point. In the cases where this is not possible, the installation of a power equipment that compensates the disturbances in real time becomes viable.

To evaluate power quality problems and propose a solution adequately, first a monitoring of voltage parameters as magnitude, phase, and frequency of the fundamental and harmonic components is required. In addition, before voltage variations can be compensated, a fast detection of them must be performed by the compensation system. Mathematical real-time estimation algorithms are crucial for both the mentioned purposes.

The Kalman filter (KF) is a mathematical method widely extended in many areas of science, and has important applications in the power quality field of electrical engineering. Some of the most important are discussed in this chapter. First, some power quality compensators and the usual requirements of the supply voltage in electrical systems are addressed, to have a clear view of the applications. Then, the applications of the KF as detector of disturbances, and as estimator of parameters used in monitoring are discussed.

2. Active power compensators for improving power quality

Numerous power electronics topologies have been proposed for the compensation of disturbances in electrical systems (Bollen, 2000), (Dugan et al., 2003), (Martínez, 1992), (Sannino et al., 2000), (Zamora, 1997). Among the most important to compensate sags, swells, and interruptions are: the uninterruptible power supply (UPS), static transfer switch (STS), dynamic voltage restorer (DVR), and the transformer with changeable taps. A brief operative description of the aforementioned equipments is given next, in order to relate the applicability of the KF. A detailed description of the compensators, as well as more kinds that are focused in correcting other disturbances can be consulted in the above references.

Uninterruptible power supply (UPS) – it is considered one of the best options of power compensators. It consists of an ac/dc converter (controlled rectifier, uncontrolled rectifier or active front-end rectifier), an energy storage bank (frequently based on batteries), and a dc/ac converter (inverter). The UPS is very common and is very extended worldwide in low, medium, and high power levels. It keeps a constant and regulated voltage at the load, even under eventualities as sags and interruptions (with backups going from a few cycles to several minutes). A basic scheme of the UPS is shown in Figure 1. This scheme in particular can be operated in online or offline mode. The online mode consists in feeding the load directly from the inverter (when the ac mains is present it works with the rectifier, and when it is not it works with the batteries), and if it fails, the static switch changes the connection to the source. The offline mode consists on maintaining the load connected to the source permanently, and when a disturbance appears, the switch changes the operation to the inverter. An algorithm to detect the presence of a sag or an interruption in real time is needed to manage the operation of the equipment and protect the load effectively, particularly in offline systems. The speed of detection and the corrective action together have to be smaller than half cycle of the sinusoidal voltage wave, since the majority of critical loads can not tolerate a disturbance during a greater time.

Static transfer switch (STS) – under an eventuality, this equipment based on static switches disconnects the load from the disturbed source and transfers it to another source with good conditions, or to a small generation plant. The approach is applicable and effective for low and medium voltage at distribution level. The two sources must be really independent and synchronized correctly. It requires fast detection of disturbances too, to coordinate the transfer. Figure 2 shows a general scheme of the STS.

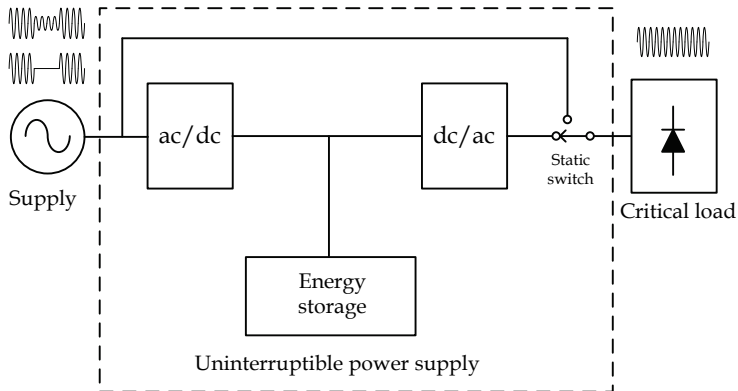


Fig. 1. A basic scheme of the uninterruptible power supply (UPS).

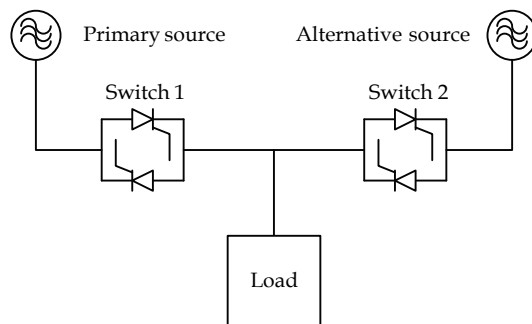


Fig. 2. Static transfer switch (STS).

Dynamic voltage restorer (DVR) – this compensator has received special attention recently. Depending on the topology, it can provide protection against sags and swells in low, medium, and high voltage levels (Affolter & Connell, 2003), (Joos et al., 2004), (Nielsen et al., 2004), (Wunderlin et al., 1998). This solution has already been used at high power levels in countries such as the United States, Israel, Japan, United Kingdom, and Singapore for the protection of complete industrial facilities. Figure 3 shows a basic scheme of the DVR. It consists of a power inverter connected in series between the source and the load through a coupling transformer, having also an energy storage element. When a disturbance appears, the equipment injects the missing or exceeding voltage in series in such a way that the load always has a constant and regulated voltage. The DVR also requires a disturbance detection algorithm with the aim of coordinating the change in the reference to inject.

Transformer with electronic tap changers – it uses static switches to change the turns ratio of a transformer dedicated to a single load or of a distribution transformer, under voltage variations (Baitech & Barr, 1985), (Hingorani & Gyugyi, 2000), (Fletcher & Stadlin, 1983), (Sannino, 2000). It is a solution that maintains the voltage regulation within a tolerance band, generally between 90% and 110%. The secondary coil is divided into various sections, which are connected or disconnected by the switches. It also requires a method that monitors the thresholds of voltage in a fast way. Figure 4 illustrates the device.

It is evident that the compensation equipments abovementioned require a fast method to monitor and detect voltage variation disturbances. A fast detection is crucial for the equipment to be effective, and to accomplish its operation of compensating the disturbance as fast as possible. The KF, among other methods, is a valuable tool for this purpose. But, to design a correct algorithm, it is necessary to know the limits on the requirements of the supply voltage for critical loads, a topic discussed in the following section.

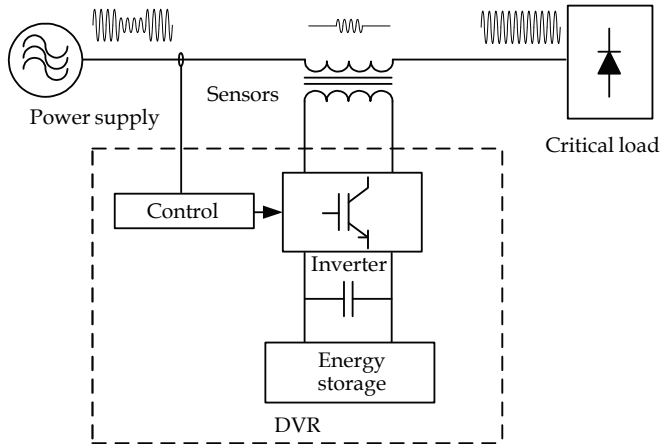


Fig. 3. Dynamic voltage restorer (DVR).

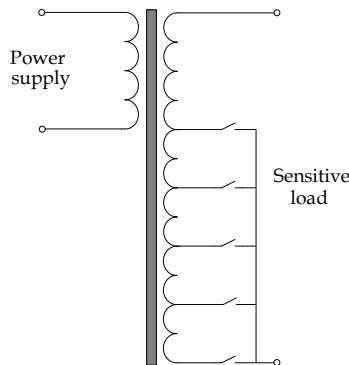


Fig. 4. Transformer with electronic tap changers.

3. Requirements of the supply voltage for critical loads

Requirements of the supply voltage for specific critical loads are shown in Table 1 (Martínez, 1992). The majority of low critical loads allow slow and steady state voltage variations within $\pm 10\%$ of the nominal voltage. Nonetheless, some highly critical loads only allow variations within the $+5\%$ and the -8% , or even within $\pm 5\%$. Similar requirements are established in (IEEE Std 1100-2005, 2006). In general, the tolerance in magnitude is greater for fast voltage variations, during short lapses of time. As with the steady state case, the

requirements for transient events are stricter for highly critical loads. These are general outlooks, but specifically, each load has its own susceptibility profile of failure regarding magnitude of voltage variations vs. duration.

Nowadays, there is a standard susceptibility graphic for equipments of information technology, computer equipment, copy and fax machines, and other electronic equipment. This is the CBEMA curve (IEEE Std 1100-2005, 2006). It reflects the magnitude tolerances of voltage variations vs. duration for the aforementioned equipments. The first version of this curve was proposed in 1977 by the Computer and Business Equipment Manufacturers Associations (CBEMA). Since then, the curve has been widely published and used in the literature. It was updated in 1996 and revised in 2000 by the Information Technology Industry Council (ITI), and is now an essential part of the standard 1100 of the Institute of Electrical and Electronics Engineers (IEEE).

The curve has been improved to the point that today it is a representative standard for modern computer equipment, and it is frequently used in the power quality field as a performance guide for loads in general, although not all the equipment manufacturers make their designs to meet the tolerance shown in it, and even though this curve does not reflect an absolute profile for all kind of loads, but only for the informatics and computing equipment. Figure 5 shows the CBEMA graphic. If the coordinates of magnitude vs. duration of a voltage variation fall outside the tolerance zone, the event could cause problems. For example, the graphic allows a +200% variation for an event lasting 1ms; and permits a limit up to +500%, but for short impulses below 100 μ s .

Characteristic	Requirements of little critical loads	Requirements of very critical loads
Stability of voltage at steady state	+10% -10%	+5% -8%
Stability of voltage at transient state	+20% -30% ($\leq 40ms$)	+20% -30% ($\leq 4ms$)
Short outages of less than 10ms	No disconnection but can generate errors	Disconnection exists and generate errors

Table 1. Requirements of the supply voltage for critical loads.

On the basis of this graphic, an algorithm that determines the existence of an electrical disturbance when the voltage surpasses a tolerance band (for example of $\pm 6\%$) can be proposed, with the aim of controlling the corrective action of power quality compensators.

4. Detection of electrical disturbances with the Kalman filter and the digital RMS algorithm

4.1 Previous works on detection of electrical disturbances

It is evident that to perform correcting actions in an electrical system, an algorithm that detects the start of disturbances is necessary, as this action governs when a compensating device begins operating. Several methods for these purposes have been published, with different advantages and drawbacks. Among the most used, and relevant detection and estimation techniques are: space vector PWM (SVPWM) (Wang et al., 2004), fast Fourier transform (FFT), DQ transformation (Montero & Enjeti, 2005), symmetrical components

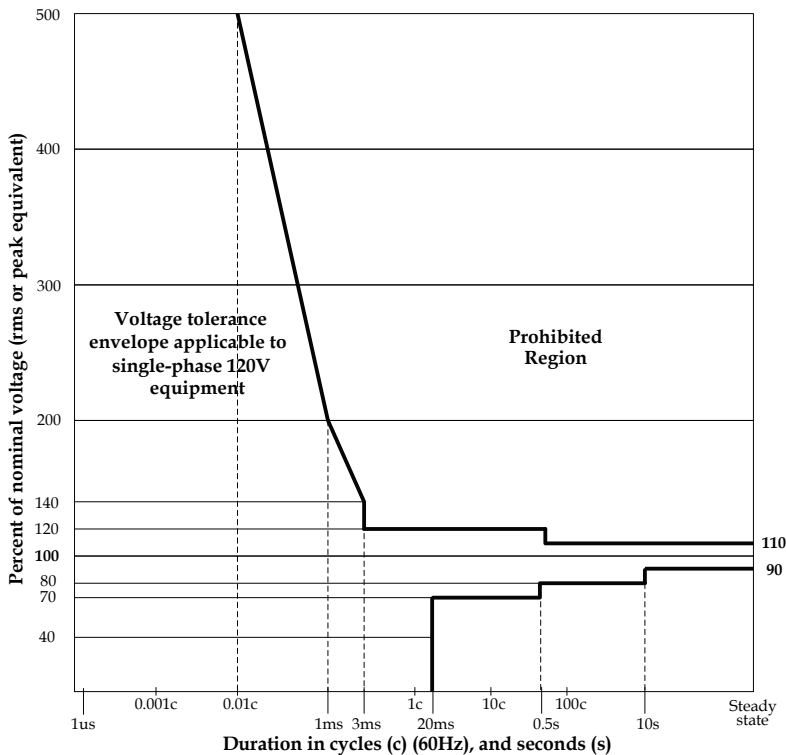


Fig. 5. ITI (CBEMA) curve (2000). Profile graphic of voltage variation vs. admissible time in the supply of modern electronic and computer equipment.

method, Kalman filter (Ma & Girgis, 1996), (Vilathgamuwa et al., 2003), (Yu et al., 2005), (Schwartzenberg et al., 1994), rms of the error vector (Nielsen et al., 2004), peaks detection (Fitzer et al., 2004), numerical matrix method (Fitzer et al., 2004), digital RMS calculation (Bollen, 2000), (Deckmann & Ferreira, 2002), and wavelet transform (Saleh & Rahman, 2004), (Dash et al., 2001).

The FFT process has slow performance due to the one cycle window requirement. The peaks detection method can take up to half cycle to detect a disturbance and the noise can detriment the performance. The numerical matrix method has response times around 7ms and the operation is sensible for high sampling rates, conducting to errors.

The method in (Dash et al., 2001) uses spline wavelets to detect the beginning and end of disturbances, and KF at steady state condition to classify and give information of the disturbance, such as frequency, depth, and phase (the KF is not used for detection). In addition, the dependence of the speed of the wavelets method on the starting phase angles of the disturbance is not considered. In fact, slow results can be obtained at some of them. Besides, the method does not take into account the influence of voltage harmonics. Their presence can guide to slower and less reliable detections.

One advantage of using the DQ transformation as in (Montero & Enjeti, 2005) and (Nielsen et al., 2004) is that only one algorithm is needed to monitor a complete three phase system.

However, the loss of information due to the three to one mapping gives more disadvantages. The method can become too slow, having a wide time range of detection, depending on the depth of the voltage variations, the simultaneousness of them on the three phases, and the electrical angles at which they appear. Moreover, if the system has harmonics, the algorithm must be configured to perform slower in order to be reliable, having then high probabilities of very slow detections.

Two of the fastest, with more advantages, and most used methods are the KF and the digital online RMS algorithm. The KF as applied in (Schwartzberg et al., 1994) is used only for prediction of the future behavior of the signal at N samples in the future, to use it as part of a control system. It is not used for detection of disturbances. The signal is modeled taking n harmonics into account, but the main disadvantage is the high processing time consumption due to the big extension of the model.

In fact, the KF is applicable to help some active power compensators, by playing the roll of online detector of electrical disturbances, mainly of sags, swells, and interruptions. The detections are required to be as fast as possible, in order to give the compensator the command that will start the corrective action. The KF is a good candidate since it can be fast. However, it suffers slowness in estimations in some specific cases. In reality, as will be realized, the KF can be combined with another method to eliminate its drawbacks.

A fast detection algorithm for sags, swells, and interruptions based on the combination of the digital RMS technique and the KF, called the KF-RMS method, is addressed in section 4.4 (González et al., 2006), (González et al., 2008). The slow detection speeds the KF has at some regions are eliminated by the RMS algorithm, and the fast speeds it has at other regions are availed. A complete study and a range of detection times are derived, assuring high probabilities that detections of disturbances are very fast. The KF-RMS algorithm is faster than many algorithms and considers all possible starting angles of disturbances, all depths, voltage increases, and a voltage polluted by harmonics; thus considering all the cases, and not only particular approaches. Experimental tests are also discussed in section 4.6.

4.2 The Kalman filter as voltage estimator and detector of disturbances

The ideal case

In order to make an estimation of the rms value of a voltage with the KF, the following development can be made. If only the fundamental component of the voltage is considered to derive a model for the KF, it can be started from the following digitalized expression:

$$v[kT] = b_1 \sin[\omega kT + \phi] \quad (1)$$

where b_1 is the nominal peak value of the voltage, k is the sample number, and T is the sampling period. It can be decomposed as:

$$v[kT] = b_1 \cos \phi \sin[\omega kT] + b_1 \sin \phi \cos[\omega kT] \quad (2)$$

If the states are chosen to be $x_1 = \frac{b_1}{\sqrt{2}} \cos \phi$ and $x_2 = \frac{b_1}{\sqrt{2}} \sin \phi$, then the state space model can be expressed as:

$$\mathbf{X}_k = \mathbf{A}\mathbf{X}_{k-1} + \mathbf{W}_{k-1} = \begin{bmatrix} x_1 \\ x_2 \end{bmatrix}_k = \begin{bmatrix} 1 & 0 \\ 0 & 1 \end{bmatrix} \begin{bmatrix} x_1 \\ x_2 \end{bmatrix}_{k-1} + \begin{bmatrix} w_1 \\ w_2 \end{bmatrix}_{k-1} \quad (3)$$

where w_1 and w_2 allow the state variables to randomly move in time. It should be noted that at normal conditions (no phase-shift), the state x_1 has the maximum value $b_1/\sqrt{2}$ (rms value) whereas x_2 is zero. Then, the measurement matrix can be defined as:

$$\mathbf{H}_k = \begin{bmatrix} \sqrt{2} \sin[\omega kT] & \sqrt{2} \cos[\omega kT] \end{bmatrix} \quad (4)$$

which must be synchronized with the source voltage. Next, the following well-known KF matrix equations are computed recursively at every sample:

$$\mathbf{X}_k = \mathbf{A}\mathbf{X}_{k-1} \quad (5)$$

$$\mathbf{P}_k^- = \mathbf{A}\mathbf{P}_{k-1}^+ \mathbf{A}^T + \mathbf{Q}_k \quad (6)$$

$$\mathbf{K}_k = \mathbf{P}_k^- \mathbf{H}^T (\mathbf{H}\mathbf{P}_k^- \mathbf{H}^T + \mathbf{R})^{-1} \quad (7)$$

where \mathbf{P}_k^- is the prior estimate of the error covariance matrix, and \mathbf{K}_k is the optimal Kalman gain matrix, which improves the estimation at every sample. Then a measurement is taken:

$$y_k = \mathbf{H}\mathbf{X}_k + v_k \quad (8)$$

where y_k is the sample and v_k is the noise of the measurement.

In KF, a prior estimate of the system at sample k , denoted by \mathbf{X}_k^- , is used to derive an updated estimate \mathbf{X}_k^+ based on the measurement y_k . This estimate is computed with:

$$\mathbf{X}_k^+ = \mathbf{X}_k^- + \mathbf{K}_k(y_k - \mathbf{H}\mathbf{X}_k^-) \quad (9)$$

And finally, the updated estimate of the error covariance matrix, based on its prior estimate is calculated:

$$\mathbf{P}_k^+ = (\mathbf{I} - \mathbf{K}_k \mathbf{H}) \mathbf{P}_k^- \quad (10)$$

The covariance matrix \mathbf{Q} of w is given by:

$$E[w_i w_j^T] = \begin{cases} Q_i & i = j \\ 0 & i \neq j \end{cases}, \text{ or } \mathbf{Q} = \begin{bmatrix} Q_1 & 0 \\ 0 & Q_2 \end{bmatrix} \quad (11)$$

and the covariance of v is $\mathbf{R} = R$. The signs + and - at all expressions are used to denote the times immediately before and immediately after a sample is taken.

Figure 6 shows the KF estimation of the rms value of an ideal sinusoidal voltage (without harmonics neither noise) with nominal value $b_1 = 179.6V$ ($127V_{rms}$), in which a $0.4p.u.$ sag (remaining $0.6p.u.$ in the voltage) occurs at $t = 1s$.

As with many other algorithms, the KF has a trade-off: the speed can be improved but the cost is the insertion of high overshoots during transient response; or the estimation can be performed softly and without overshoots, but having a slower response in consequence. The values of the state variances in this case are chosen as $Q_1 = Q_2 = 0.004$, to obtain a reasonable fast speed in the estimation without having transient overshoots. Realize that the estimation of interest is only the one given by x_1 , and that x_2 has no useful information. x_1 has a fast and flat response.

It takes about $9ms$ to get the new valid value at steady state. Nevertheless, together with the KF estimation, thresholds of $\pm 6\%$ and -6% of the reference value $b_1/\sqrt{2}$ can be used to make the detection of the disturbance in a much shorter time. When the estimation x_1 gets outside this range, then the sag is detected. Detection time in this way is only $1.7ms$ (very fast) and a pulse shows the moment of detection in the third graph (zoom). The thresholds are set to $\pm 6\%$ in order meet the CBEMA guidelines of voltage supply, which establishes the limit at $\pm 10\%$, allowing normal voltage variations and having shorter times of detection. Note that there is also a trade-off in the selection of this tolerance band. The smaller it is, the more susceptibility for false detections, and as greater it is, less susceptibility.

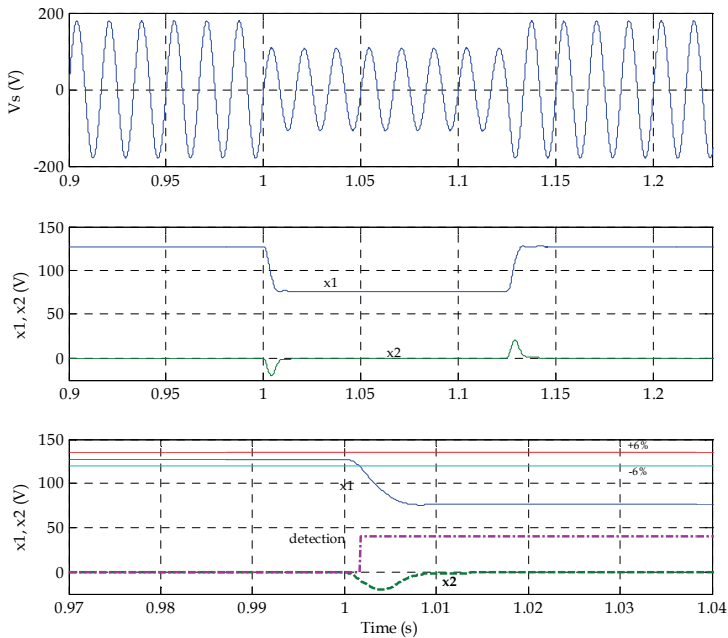


Fig. 6. Estimation with the KF of the rms value of an ideal supply voltage with nominal value $127V_{rms}$. A $0.4p.u.$ sag occurs at $t=1s$, and its detection is shown.

The case with harmonics

The previous example of voltage is impossible to find in practice. These results of detection speed and flatness will never be exactly reproduced in the estimation of a real voltage. Voltage supply, even at residential facilities has the presence of harmonic distortion, and the situation could be much marked at industrial environments. Hence, a more practical and useful algorithm for detection of disturbances must consider a non clean voltage.

Numerous authors have proposed models of the KF to make estimations with harmonic distortion. Some examples are shown in (Girgis et al., 1991), (Schwartzenberg et al., 1994), (Ma & Girgis, 1996), (Yu et al., 2005). This can be made considering the harmonic terms in the signal:

$$v[kT] = b_1 \sin[\omega kT + \phi_1] + b_3 \sin[3\omega kT + \phi_3] + b_5 \sin[5\omega kT + \phi_5] + b_7 \sin[7\omega kT + \phi_7] + \dots, \quad (12)$$

and deriving the KF model with all the components. The great advantage of doing this is that the magnitudes of each harmonic component can be calculated online separately, and can be used for monitoring. However, this makes the model (3) very big, with two states for each harmonic that is considered. E.g. if four harmonics were established, the dimension of the model would be 10. So the matrix operations involved in the KF become bulky, and the algorithm becomes impractical. The computational load itself can take a lot of time.

An approach to overcome this is by using the original model that considers only the fundamental component in (3) and (4), but managing it in such a way that it can work reasonable well in the presence of harmonics. The KF model based on only the information of the fundamental component has the benefit of high speed estimation, but it becomes oscillatory if the system has harmonics. The method can be manipulated to give higher speed, and also to give less oscillation on the estimation of x_1 , by giving more weight to the state variance Q_2 of x_2 than to the state variance Q_1 of x_1 . In this way a greater part of the oscillation (caused by harmonics) of the estimation is "sent" to x_2 .

Figure 7 shows an example of the estimation with KF of the rms value of a voltage that is disturbed with a $0.4p.u.$ rectangular sag at $t=1s$, and that has the following magnitudes of harmonics ($THD = 11.84\%$): $b_3 = 0.020b_1$, $b_5 = 0.100b_1$, $b_7 = 0.050b_1$, $b_{11} = 0.030b_1$, and $b_{13} = 0.015b_1$; with the fundamental component as $b_1 = 179.6V$ ($127V_{rms}$). These magnitudes of harmonics are selected to take above the worst THD case allowed in the standards IEC 61000-2-2 for low voltage, and IEC 61000-3-6 for medium and high voltage power supply systems (which are set to 8%); and above the recommended limits in the IEEE Std 519-1992 (which are set to 5% for low voltage, 2.5% for medium voltage, and 1.5% for high voltage systems). This represents a tough and highly distorted condition to test the algorithm, really giving it high usefulness for real practical systems. The state variances are now set to $Q_1 = 0.0009$ and $Q_2 = 0.0625$. These values of Q give an adequate speed with low oscillation in the x_1 estimation.

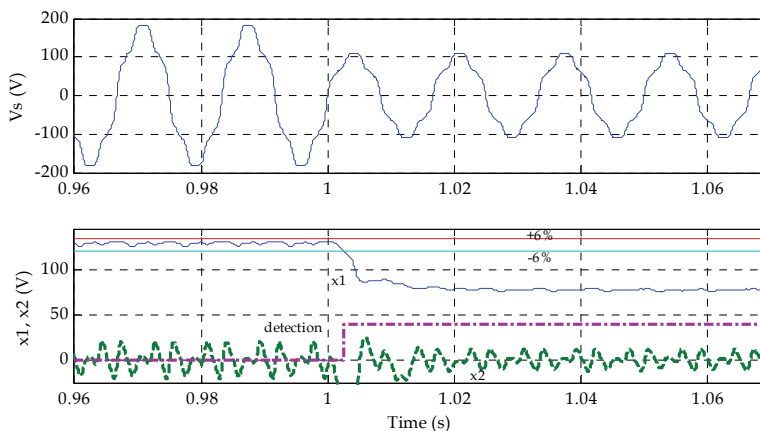


Fig. 7. Estimation of the rms value of a distorted supply voltage with the KF. The detection of a $0.4p.u.$ sag is also shown.

Although there is a little oscillation on x_1 , it can be noted that a greater part is sent to x_2 . In this case, x_1 takes about $14ms$ to get the new valid value. As with the ideal case, the same thresholds of $+6\%$ and -6% of the reference value $b_1/\sqrt{2}$ are used to detect the disturbance. The little oscillation is allowed by this tolerance band satisfactorily. Detection time in this case is $2.6ms$ and a pulse shows the moment of detection. The estimation speed has to be slightly decreased than in the ideal case, to have a more reliable estimation that involves the harmonic distortion of the measured supply voltage, allowing a correct disturbance detection. This behavior is good enough to have an useful algorithm with low processing work, fast, and with easy implementation.

Consideration of the starting angle of the disturbance in the Kalman filter algorithm

The previous examples showed the beginning of the event at $t = 1s$ in a 60Hz system, i.e. at an angle of 0° of the signal. The dependence of the estimation speed of the KF with the electrical angle at which the disturbance appears, and the presence of the harmonics listed in the previous example, are considered in the following analysis.

Figure 8 shows a graphic of detection time vs. starting angle of a rectangular sag of $0.4p.u.$, considering the harmonics. It can be observed that at some regions of phase the KF is very fast (less than $1ms$), but at others, slow detections are experienced. For instance note that at 100° the detection time is around $6ms$, whereas at 70° it is much less than $1ms$. The range of detection for sags of $0.4p.u.$ is $0.18ms \leq t_d \leq 6.10ms$. It is important to consider all the cases in an algorithm, to evaluate if it is really going to be fast at all circumstances. Numerous authors have reported fast speeds with other algorithms or even with the KF, but actually show results at favourable angles that give fast estimations. This is evident in Figure 8.

The detection times that can be obtained, considering the previously mentioned levels of harmonics and the starting angle of the disturbance, result in a wide range of values. The digital RMS algorithm is other of the methods that give very good performance with relatively high speed. This method can be used to help obtaining faster estimations at the regions the KF shows slowness. The performance of the RMS method is addressed next, and then how it can help the KF, in a unified method, in the following section.

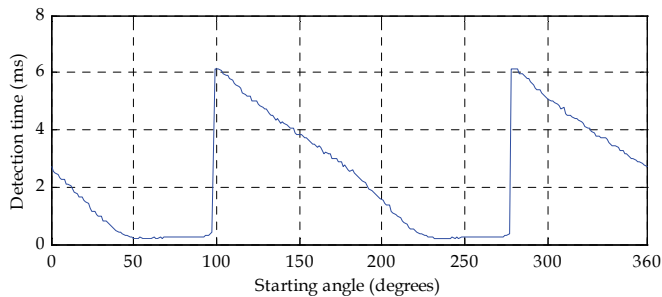


Fig. 8. Detection time vs. starting angle of a $0.4p.u.$ rectangular sag using the KF.

4.3 The digital recursive RMS calculation method as detector of disturbances

The expression for the well-known online digital RMS calculation is given by:

$$V_{RMS}[k] = \sqrt{\frac{1}{N} \sum_{i=k-N+1}^k v^2[i]} \tag{13}$$

where N is the sliding window size for the computation, k is the number of sample, and v_i are the samples. There are two kinds of application, the one cycle window, and the half cycle window. The method needs N to be an integer multiple of one cycle or of a half cycle, in order to avoid oscillations on the estimation. A recursive alternative to spend less processing time can be found in (González et al., 2006). It provides a significant processing time saving when N is large. The RMS method has the advantage of providing a very flat estimation, even if there are harmonics in the voltage, which translates into reliability.

The one cycle RMS technique takes one cycle in giving a valid result for a change in the voltage, and the half cycle RMS method takes a half cycle. However, if inferior and superior thresholds are also defined around a reference voltage, both window sizes can be used for a faster detection of disturbances when the estimated voltage value gets outside them. As the half cycle RMS takes less time to get to a new value on transitions, it is clear that it is also faster to detect disturbances when using thresholds. Thus, it is used in the following, also with the thresholds of $\pm 6\%$ around the reference voltage to meet the CBEMA guidelines, and to allow faster detections, as selected for the KF.

Figure 9 shows the calculation of the rms value of the voltage of the same example shown for the KF ($0.4p.u.$ sag, with the same harmonics: $b_3 = 0.020b_1$, $b_5 = 0.100b_1$, $b_7 = 0.050b_1$, $b_{11} = 0.030b_1$, and $b_{13} = 0.015b_1$, with $b_1 = 179.6V$ ($127V_{rms}$)), but now using the half cycle RMS method. The estimation takes half cycle to get to the new valid value, but detection time is $2.8ms$, a very similar result than the one of the KF. A pulse shows the moment of detection. Note that the estimation is soft and flat, even with the considered harmonics.

Consideration of the starting angle of the disturbance in the RMS algorithm

The speed of this method is found to be dependant on the starting angle of the disturbance too. Figure 10 shows the graphic of detection time vs. starting phase angle of a $0.4p.u.$ rectangular sag (the harmonics of the previous examples are considered too). At some regions the method is slow and at others is fast, but not with marked behavior as the KF. The detection range for a $0.4p.u.$ sag is $0.79ms \leq t_d \leq 3.96ms$.

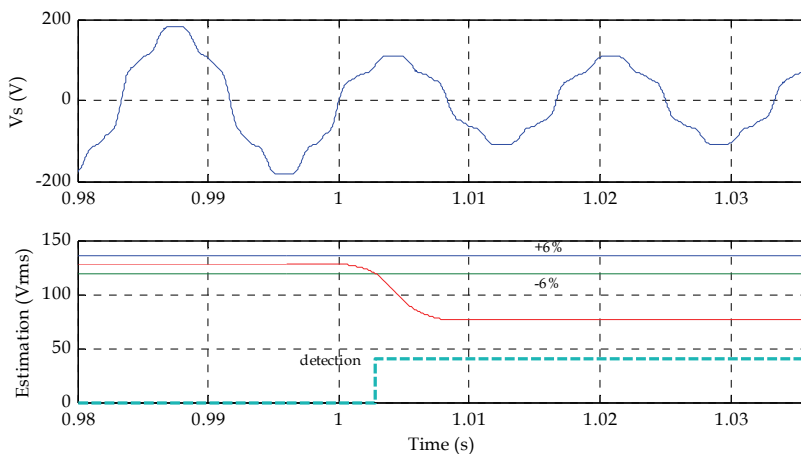


Fig. 9. Estimation of the rms value of a distorted voltage with the digital RMS algorithm. The detection of the occurrence of a $0.4p.u.$ sag is also shown.

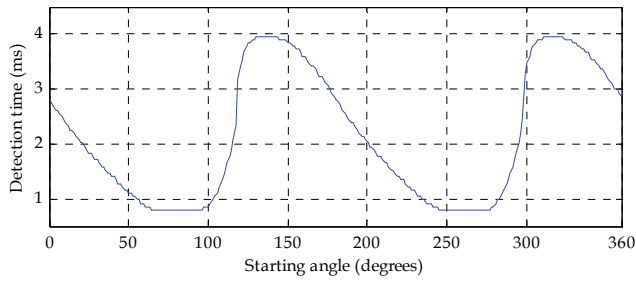


Fig. 10. Detection time vs. starting angle of a $0.4p.u.$ sag, using the digital RMS algorithm.

4.4 Method for detection of disturbances based on the combination of the KF and RMS algorithms: the KF-RMS method (González et al. 2006), (González et al. 2008)

The graphics speed of detection vs. starting angle of a $0.4p.u.$ sag of the KF and RMS methods are shown together in Figure 11. Observe that in some cases, depending on the starting angle of the disturbance, the KF is faster than the RMS, whereas in other cases the RMS is faster. This graph leads to the proposal of the KF-RMS method, based on the combination of the KF and the digital half cycle RMS algorithm. The central idea can be noticed by observing the advantages and drawbacks of speed of each one of them. The method consists on monitoring with the online execution of both algorithms simultaneously, and taking the decision of the one that first detects the disturbance (logic OR of detecting signals). Figure 12 shows the resultant graphic for the KF-RMS method.

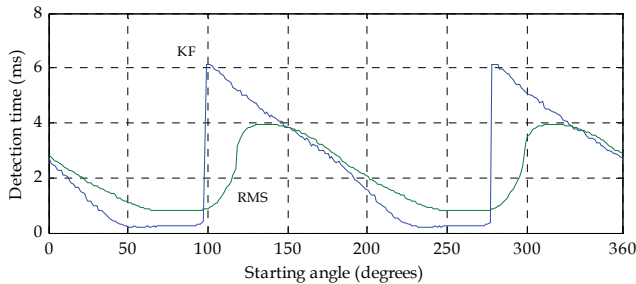


Fig. 11. Detection time vs. starting angle of a $0.4p.u.$ rectangular sag, occurring in a signal distorted by harmonics. Both KF and digital RMS algorithms are shown.

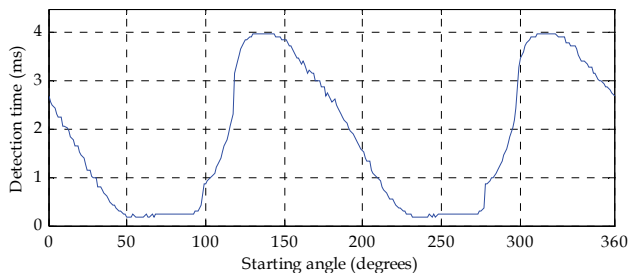


Fig. 12. Detection time vs. starting angle of $0.4p.u.$ rectangular sag occurring in a distorted voltage signal, with the KF-RMS method.

In this way, very fast detections are obtained with the KF, and the regions at which it is slow are rejected by the RMS method. Detection time is now between $0.18ms$ and $3.96ms$, which clearly falls in less than a quarter of cycle of $60Hz$ systems. However, this is only valid for $0.4p.u.$ rectangular sags, since all depths are not considered.

A very few authors have considered the dependence of speed of the KF and the RMS methods on the depth and on the starting angle of the disturbance together, and the small amount that consider it, do not consider a voltage distorted by harmonics. Considering all these aspects is crucial as a validation of one reliable method at all possible events can be obtained, not only for particular cases. Hence, to make a generalization, 3D graphics are developed next. The detection time, the angle at which the disturbance begins, and the sag depth are considered. The high levels of voltage harmonics addressed in the previous sections are also considered.

Figure 13 shows the corresponding 3D graphic for the KF method. The analysis considers depths from $0.1p.u.$ to $1.0p.u.$ (complete interruption). The same behavior of Figure 8 can be noted, but it can be seen that as the depth increases, the detection becomes faster. At all depths the method is fast at some regions of angles, while at others it is slow, as with the $0.4p.u.$ sag case. Note that the maximum detection time is $9ms$, which is a high value of time (more than half cycle). If a sag occurs near these regions the method performs slowly. Considering all points, the KF method has a range of detection times of $0.061ms \leq t_d \leq 9ms$.

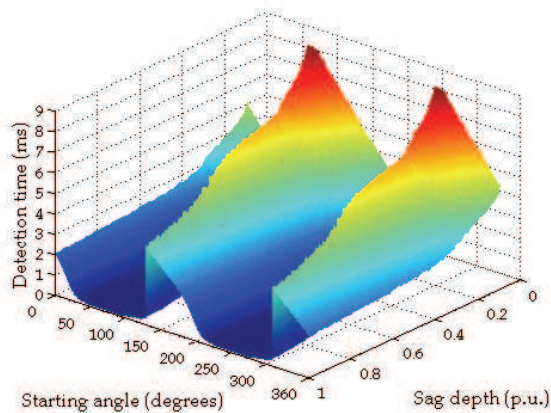


Fig. 13. Detection time vs. starting angle vs. sag depth with the KF algorithm.

Figure 14 shows the 3D graphic for the RMS algorithm. The same behavior as in Figure 10 is observed at all depths too, and the detection speed also increases with depth. The method has a detection time range of $0.48ms \leq t_d \leq 6.9ms$.

If the KF-RMS algorithm is executed, the 3D graphic of Figure 15 results. Observe that the advantage of fast detections in some regions of KF is availed, and the regions at which KF is slow are rejected by the RMS method. The range for detection in general is now $0.061ms \leq t_d \leq 6.9ms$. Figure 16 shows the same graphic but with a plane that represents the quarter of cycle ($4.16ms$ at $60Hz$). It can be seen that the majority of the events are below this time. Extracting probabilities from all the points, it can be established that, for rectangular sags between $0.1p.u.$ and $1.0p.u.$, and supposing that all the points come out with the same

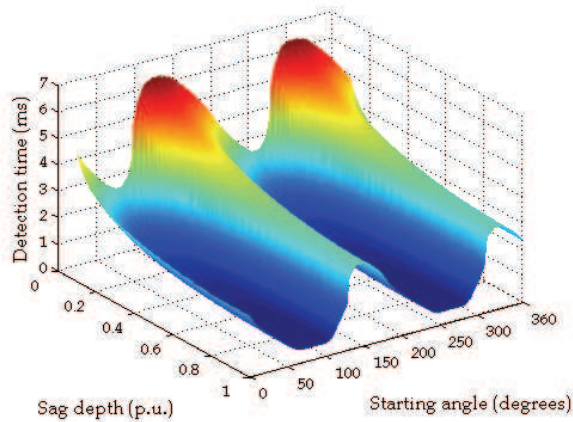


Fig. 14. Detection time vs. starting angle vs. sag depth with the digital RMS algorithm.

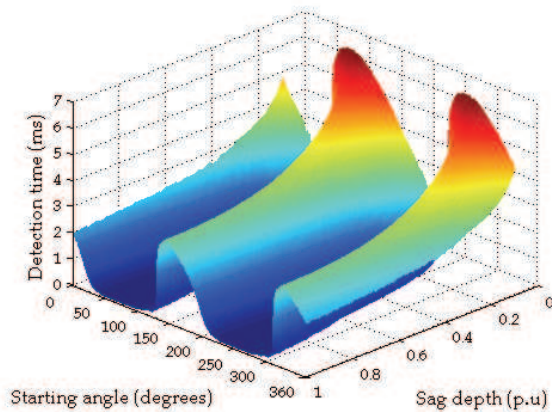


Fig. 15. Detection time vs. starting angle vs. sag depth with the KF-RMS algorithm.

recurrence (in practical systems short sag depths are more probable), the KF-RMS algorithm has the following properties:

- Range of detection: $0.061ms \leq t_d \leq 6.9ms$. In a distorted environment: $THD = 11.84\%$
- $prob(t_d > 4.16ms) = 9.04\%$
- $prob(t_d < 4.16ms) = 90.9\%$
- $prob(t_d < 2.00ms) = 56.9\%$

The method has a very high probability (90.9%) that sags and interruptions are detected in less than a quarter of cycle, and more than 50% of probability (56.9%) that they are detected in less than 2ms, which is very fast. Times a little greater than a quarter of cycle may be obtained with sags of small depth, but only at some specific regions of phase. In fact, detection times will never be equal or greater than half cycle.

All the previous analyses are made for swells. A better result, with much more favorable behavior is obtained for swells with the KF-RMS method. Figure 17 shows the corresponding 3D graphic. It can be seen that most of the events are below 2ms. The following properties are obtained for swells from 1.1p.u. to 2.0p.u.:

- Range of detection: $0ms \leq t_d \leq 6.3ms$. In a distorted environment: $THD = 11.84\%$
- $prob(t_d > 4.16ms) = 3.95\%$
- $prob(t_d < 4.16ms) = 96.04\%$
- $prob(t_d < 2.00ms) = 78.87\%$

Detection times of practically 0ms are obtained for several swell cases, leaving all the dependence to the processing time, and the probabilities are much better than for sags and interruptions.

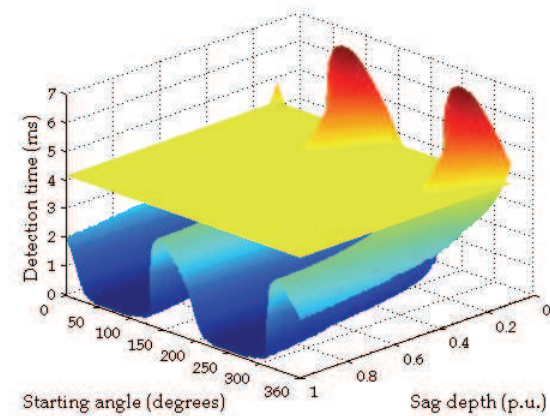


Fig. 16. Probability that sags and interruptions are detected in less than a quarter of cycle, with the KF-RMS algorithm.

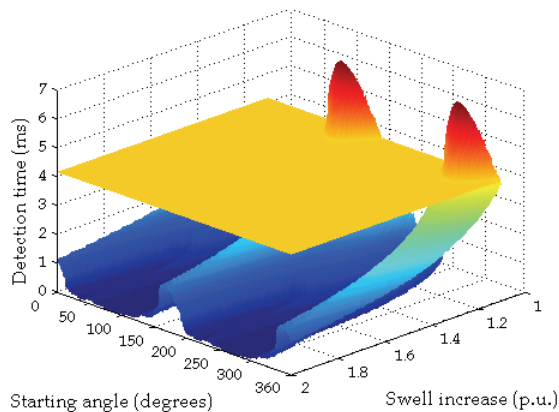


Fig. 17. Detection time vs. starting angle vs. swell increase with the KF-RMS algorithm.

The KF-RMS algorithm represents a better option for detection of voltage variation disturbances. It is important to note that the angle in which the disturbance occurs and its depth are considered in the analysis, besides of an amount of harmonic pollution that is superior to the allowed by the most important worldwide standards on voltage harmonic levels in practical electrical systems. The advantage of a very fast detection at some regions of KF is availed, and the regions at which it is slow are rejected by the RMS method.

4.5 Dependence of the KF-RMS algorithm on the sampling frequency

The previous results were derived with a sampling frequency equal to 16.384kHz and with a 60Hz supply frequency. The performance of the method also shows dependence on the sampling frequency selection. Figure 18 shows how the speed of detection is affected in both KF and RMS methods when the sampling frequency is changed, for a 0.4p.u. sag starting at 0° (including also the harmonics that have been considered through all the examples). It can be noted predominantly that the KF sees its detection speed negatively affected if the sampling frequency is reduced, whereas the RMS algorithm maintains it practically at all sample frequencies.

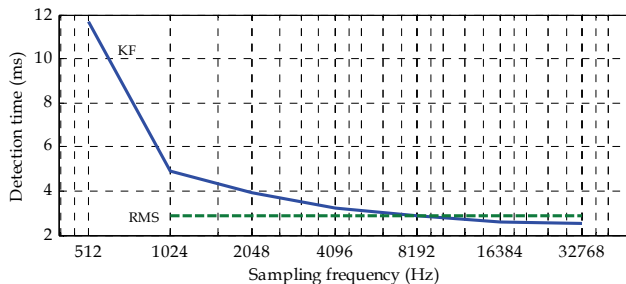


Fig. 18. Dependence of the detection time of KF and RMS methods on the variation of the sampling frequency, for a 0.4p.u. rectangular sag starting at electrical 0° .

Then, the global response of the KF-RMS method also depends on the sampling frequency. When decreased, the regions at which this method avails the high speeds of KF are lost, but the rejection of slow speeds with RMS is kept. In other words, if the sampling frequency is reduced, the behavior of the KF-RMS method will get close to the RMS one operating alone, since the global response will depend only on it. An important care must be taken when varying the sampling frequency: the RMS method must keep the number of samples of its calculation window an integer multiple of half cycle. Also, care must be taken in always keeping the Nyquist criterion satisfied on both methods (and its limit far enough) when the sampling frequency is reduced; in order to consider from the fundamental to a specific harmonic component, so aliasing does not appear that would guide to erroneous estimations. The method is found to show its main benefits and work better with sampling frequencies greater than 8.192kHz . This statement is valid if the constants of the covariance matrix \mathbf{Q} of the KF are kept fixed. Indeed, the optimal constants for one sampling frequency are not the most appropriate for others. In order to maintain the advantages of the KF-RMS method at all sampling frequencies, an adequate selection of the Q_1 and Q_2 constants is needed at each case. In this way the dependence of the KF on the sampling frequency is eliminated. Figure 19 shows that the dependence on sampling frequency is eliminated by selecting adequate Q constants. The selections are summarized in Table 2.

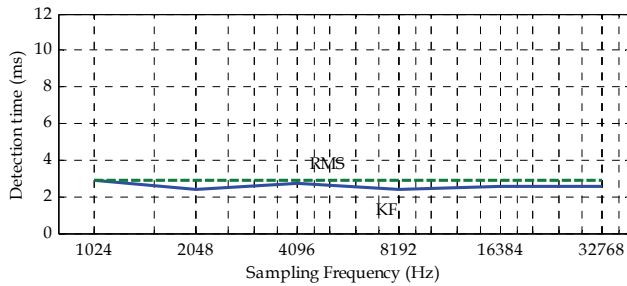


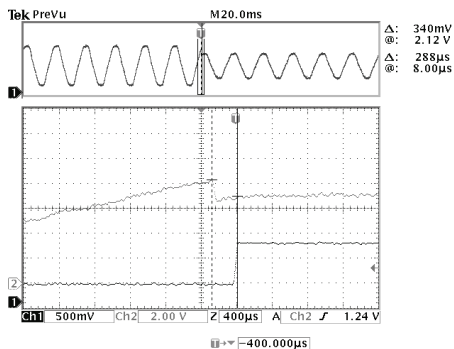
Fig. 19. Detection time of the KF and RMS methods, for a 0.4p.u. rectangular sag starting at 0°, and using adequate values Q_1 and Q_2 for different sampling frequencies.

Sampling Frequency	Q_1	Q_2
1024	1.0000	25.0000
2048	0.1296	6.2500
4096	0.0784	6.2500
8192	0.0400	3.2400
16384	0.0009	0.0625
32768	0.0169	1.0000

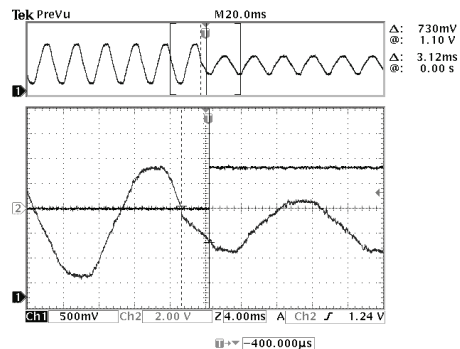
Table 2. Selection of covariance matrix constants of KF for different sampling frequencies.

4.6 Experimental tests of the KF-RMS algorithm

The KF-RMS algorithm is implemented in the Texas Instruments TMS320F2812 DSP platform. A single phase voltage signal is sampled, and scaled to 0-3V in order to use the internal ADC of the DSP. Then sags and swells of different magnitudes are emulated at the sensor. The experimental results of the KF-RMS method agree significantly with the analyses, and with the detection time graphics of Figures 16 and 17. This is proved with several generated events. Detection cases are shown in Figure 20 for sags, and in Figure 21 for swells. Very fast detection times are obtained in cases 20(a), 20(c), 20(d), 21(a), and 21(d) due to the region at which the disturbance occurs. A pulse is generated in one port pin of the DSP to show the moment of detection. The THD of the sampled signal is around 5%.



(a)



(b)

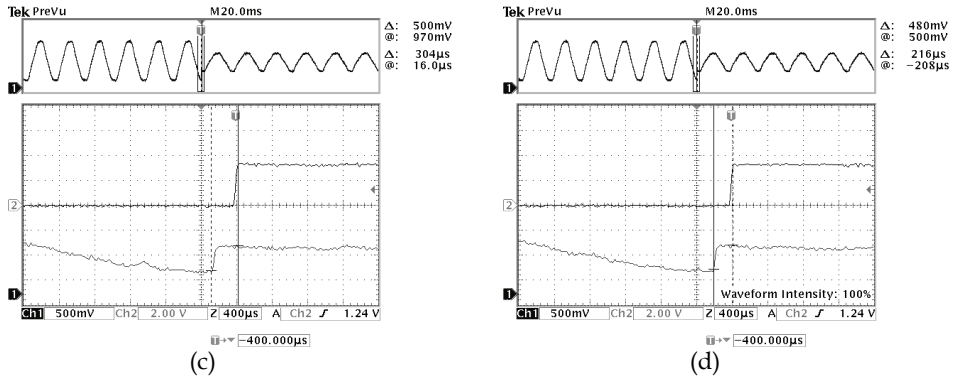


Fig. 20. Experimental detection times of the KF-RMS algorithm for sags. a) $0.4p.u.$ sag at 80° , $t_d = 288\mu s$. b) $0.5p.u.$ sag at 170° , $t_d = 3.12ms$. c) $0.5p.u.$ sag at 260° , $t_d = 304\mu s$. d) $0.5p.u.$ sag at 270° , $t_d = 216\mu s$.

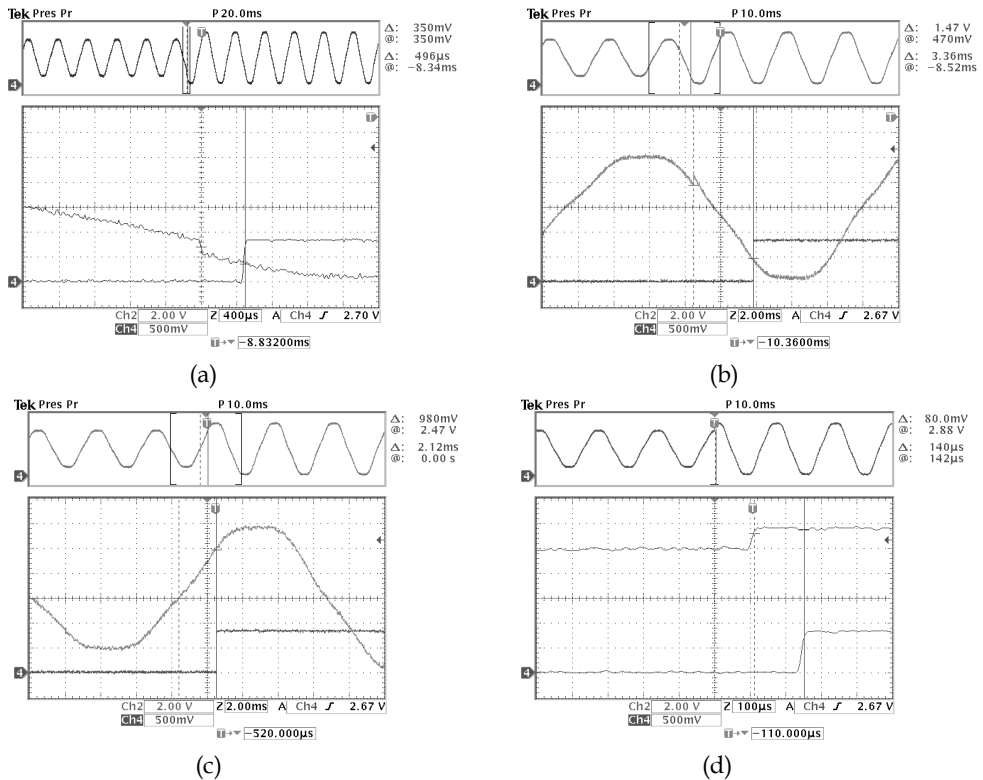


Fig. 21. Experimental detection times of the KF-RMS algorithm for swells. a) $0.4p.u.$ swell at 224° , $t_d = 496\mu s$. b) $0.4p.u.$ swell at 153° , $t_d = 3.36ms$. c) $0.4p.u.$ swell at 0° , $t_d = 2.12ms$. d) $0.4p.u.$ swell at 80° , $t_d = 140\mu s$.

5. The Kalman Filter applied for estimation of parameters in power quality monitoring of electrical systems

Another application of the KF in power quality is as estimator of parameters for monitoring purposes. Its fast real-time estimator characteristics make itself a good candidate.

Monitoring consists on obtaining information of one or more points of an electrical system, such as the behavior of a voltage or a current within a lapse of time, which can be from a few seconds to several days. This information can be recorded and used to generate the statistics of disturbances in that system, to evaluate power quality problems, and propose solutions. The information collected by voltage or current monitoring can be parameters such as magnitude, phase, and frequency of the fundamental and/or harmonic components at steady state. The number of transient disturbances within a range of time, their classifications, and durations can also be considered and recorded.

Generally, monitoring performed by most of the devices consists of four or five steps, depending of the application, and are mainly: the sampling of the signal of voltage or current of interest, the real time estimation of the magnitude, detection of disturbances, classification and characterization of the event, and compact storage of the collected data (Deckmann & Ferreira, 2002), (IEEE Std 1159.3-2003, 2004).

The voltage magnitude can be determined in a variety of ways. Many actual monitors obtain the steady state magnitude and also those of disturbances such as sags, swells, and interruptions from the digital RMS calculation (see the above bibliography and (Bollen, 2000)). Although the half cycle choice is faster, the one cycle window is frequently used. This algorithm has important advantages, such as the very flat estimation, even with the presence of harmonics, and that no matter how deep and how the shape of a disturbance is, it takes exactly a half cycle or one cycle (depending on the selected window) to reach the new valid value. This method is very useful for steady state classification of disturbances, but it only gives information related with the magnitude. Other parameters such as the fundamental frequency, the phase, and harmonic magnitudes and phases can not be interpreted. Moreover, the RMS method calculates the rms value of the signal as a whole, that is, including the fundamental and harmonic components together in the result. So, the estimation is not exactly the value of the real fundamental magnitude.

Regarding this, the KF has great advantages, as it can make the aforementioned parameter estimations simultaneously. Another method that can perform magnitude, frequency and phase estimations of all harmonic components is the Fast Fourier transform (FFT), but requires one cycle to update results. A combination of various methods can be used to obtain fast, reliable, and accurate monitoring with fast transient response. In the following, only the KF applications are assessed. Some cases of monitoring are shown, evidencing its usefulness and advantages in monitoring.

5.1 Monitoring of the fundamental component in a distorted voltage

As stated, the KF can be used for rms or peak value magnitude estimation. To classify this information in monitoring, a flat and accurate estimation is needed. At first intuition, the more complicated model with harmonics could be taken for this aim, but in fact the model that only considers the fundamental component in (3) and (4) can be used effectively, using much less processing work. In this case, as the KF is not focused for detection, but for monitoring, a different tuning of the Q matrix can be used. For instance, $Q_1 = 0.08$ and $Q_2 = 80$ are adequate values for this purpose.

Figure 22 shows the estimation of the fundamental component in a voltage distorted by harmonics (the same values that were used in the previous section are used: $b_3 = 0.020b_1$, $b_5 = 0.100b_1$, $b_7 = 0.050b_1$, $b_{11} = 0.030b_1$, and $b_{13} = 0.015b_1$, with $b_1 = 179.6V$ ($127V_{rms}$)), with the KF and also with the RMS method to compare their monitoring performances. A $0.25p.u.$ swell occurs at $t = 1s$ and ends at $t = 1.2s$ to show the transient responses. Due to the mentioned tuning of the KF, a flat estimation is achieved, similar to the one obtained with the RMS method. Note also that a very abrupt estimation change to the final value is observed, which seems to reveal the KF estimation is extremely fast. However, this is only in appearance, as the estimation actually takes about a quarter of cycle to respond from the time the disturbance occurred at $t = 1s$.

Even with this delay, the KF indeed is faster in getting the final value in this case (around a quarter cycle vs. the half cycle of the RMS), and the opposite occurs in the examples of Figures 7 and 9, i.e. the RMS gets the steady state final value first. However the goal of those cases is the detection of the disturbance. If the KF were used for detection with the tuning of this example, its detections would actually be slower than the RMS. The tuning of those examples is adequate to have a faster estimation (although with tolerable oscillations), and hence allowing faster detections.

Thus, although a very flat estimation is obtained with the KF in the application of this example, it is not as useful for fast detection of disturbances, but better for transient and steady state monitoring.

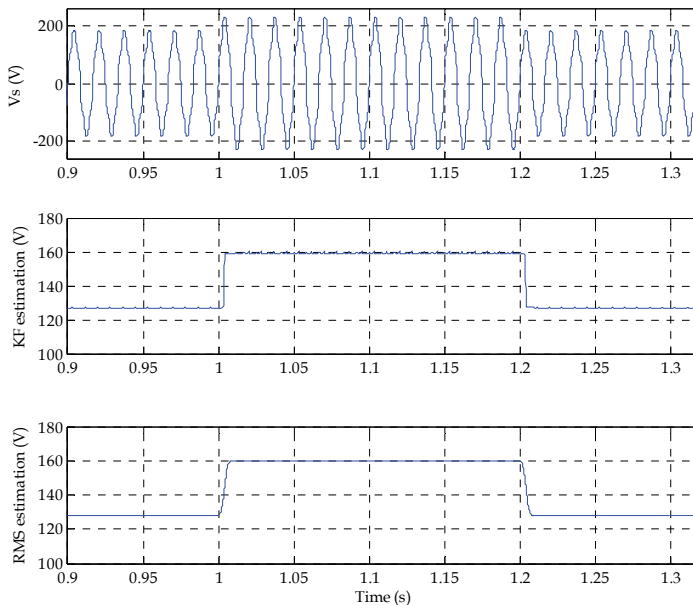


Fig. 22. RMS value estimation of the fundamental component of a distorted voltage, with the KF and RMS algorithms. A $0.25p.u.$ swell occurs at $t=1s$ and ends at $t=1.2s$.

5.2 Monitoring of the magnitude and phase of the fundamental and harmonic components

If the information of the fundamental and harmonic components is needed to monitor in an application, an extended model of the KF considering harmonics can be used. Although the computational load becomes high, the great advantage is that the magnitudes and phases of all present harmonics in a current or voltage signal can all be estimated simultaneously. The application of estimating the magnitude of harmonic components has been widely published in literature throughout many years. Some works can be seen in (Girgis et al., 1991), (Schwartzenberg et al., 1994), (Ma & Girgis, 1996), (Yu et al., 2005). An approach to estimate also the phases simultaneously is addressed next.

The KF model can be defined considering the signal with its harmonic components:

$$v[kT] = b_1 \sin[\omega kT + \phi_1] + b_2 \sin[2\omega kT + \phi_2] + \dots + b_n \sin[n\omega kT + \phi_n] \tag{14}$$

which can be decomposed as:

$$v[kT] = b_1 \cos \phi_1 \sin[\omega kT] + b_1 \sin \phi_1 \cos[\omega kT] + b_2 \cos \phi_2 \sin[2\omega kT] + b_2 \sin \phi_2 \cos[2\omega kT] + \dots + b_n \cos \phi_n \sin[n\omega kT] + b_n \sin \phi_n \cos[n\omega kT] \tag{15}$$

As with the states definition of the first example in (2), two states are now needed for each harmonic component. These can be defined as: $x_{11} = \frac{b_1}{\sqrt{2}} \cos \phi_1$, $x_{12} = \frac{b_1}{\sqrt{2}} \sin \phi_1$, $x_{21} = \frac{b_2}{\sqrt{2}} \cos \phi_2$, $x_{22} = \frac{b_2}{\sqrt{2}} \sin \phi_2, \dots, x_{n1} = \frac{b_n}{\sqrt{2}} \cos \phi_n$, $x_{n2} = \frac{b_n}{\sqrt{2}} \sin \phi_n$. Thus, the general measurement matrix can be written as:

$$\mathbf{H}_k = \begin{bmatrix} \sqrt{2} \sin[\omega kT] & \sqrt{2} \cos[\omega kT] & \sqrt{2} \sin[2\omega kT] & \sqrt{2} \cos[2\omega kT] & \dots & \sqrt{2} \sin[n\omega kT] & \sqrt{2} \cos[n\omega kT] \end{bmatrix} \tag{16}$$

Then, execution of recursive equations (5) to (10) of the KF is performed to obtain the online estimation of all the involved components. Observe that the two associated states of each harmonic are indeed the in-phase and the quadrature components of each one. The measurement matrix is synchronized with the fundamental component, but the harmonic components are rarely in phase with it in practice. Hence, the phase-shifts with respect to 0° make that both states of each harmonic share information of their actual magnitude and actual phase. One state alone can not reveal the complete information of each component. Therefore, the magnitude and phase of each harmonic can be determined with the following expressions (also online at every sample):

$$Mag_n[kT] = \sqrt{(x_{n1}[kT])^2 + (x_{n2}[kT])^2} \tag{17}$$

$$Phase_n[kT] = \sin^{-1} \left[\frac{x_{n2}[kT]}{\sqrt{(x_{n1}[kT])^2 + (x_{n2}[kT])^2}} \right] \tag{18}$$

which are accurate since the KF model that considers harmonics has the advantage that the estimation of both states of each harmonic stabilize with no oscillations. The only care in (18)

is to identify the quadrant at which the states form their vector, and add the corresponding adjustment angle. To show an example, the simultaneous estimation of the magnitude and phase of the fundamental and harmonic components of the same distorted signal of the previous example, but with different phases on the harmonics ($\phi_3 = 15^\circ$, $\phi_5 = 150^\circ$, $\phi_7 = 120^\circ$, $\phi_{11} = -60^\circ$ and $\phi_{13} = -45^\circ$), is shown in Figures 23, 24, and 25. Since the fundamental and 3rd, 5th, 7th, 11th, and 13th harmonics are considered, the dimension of the model is 12. Figure 23 shows the original signal and the estimation of the fundamental magnitude. Figure 24 shows the rest of the harmonic amplitude estimations, all in rms values. The estimation of the phases of all components is shown in Figure 25. Observe that all states take around 20ms to reach the final steady state values. The speed results are not as fast as in the previous example, due to the interaction and dependence of all components with each other in the matrix operations. However these estimations are very useful for steady state monitoring, since harmonics do not have fast changes in electrical systems. It should be noted that all the parameters are estimated online and simultaneously, and that all the delivered estimations are flat and accurate. The monitoring of harmonics in a point of an electrical system is a very common practice in power quality, and can be used to solve a variety of problems they cause.

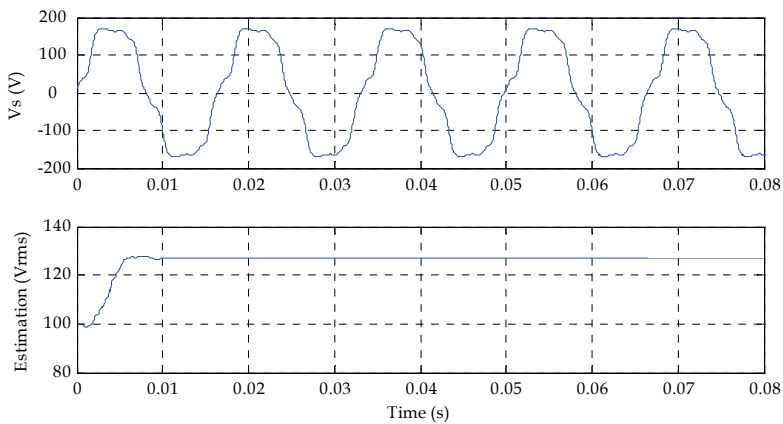


Fig. 23. Estimation of the fundamental component of the voltage signal with harmonics. The complete model that considers the fundamental and harmonic components is used.

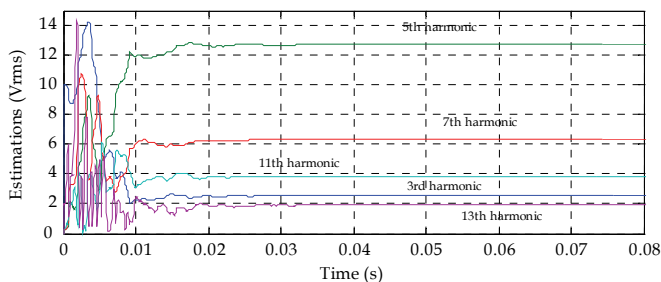


Fig. 24. Magnitude estimation of the harmonic components of the distorted voltage.

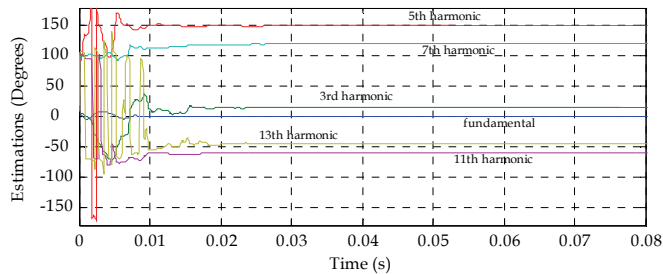


Fig. 25. Phase estimation of the harmonic components of the distorted voltage.

Other parameter that can be estimated with the KF is the frequency of a signal. One approach that estimates the magnitude, phase, and frequency of a signal simultaneously is discussed in [Dash et al., 2001], using an extended complex Kalman filter (ECKF). In fact, the estimation of all the mentioned parameters can be made simultaneously, another different parameter can be estimated, or any other combination of parameters can be extracted with the KF. The main problem is the model definition, which must be proposed adequately to have the desired estimations.

6. Conclusions

The main applications of the Kalman filter in the power quality field of electrical engineering are discussed in this chapter.

Due to its high-quality characteristics as estimator, the KF can be applied as an algorithm that is part of the control stage of some active power compensators to fast detect in real time voltage disturbances, mainly sags, swells, and interruptions. Detection of disturbances on an ideal voltage and on a more realistic case with harmonics are evaluated and compared. A simple low order KF model that considers the influence of harmonics in the signal is discussed and validated. The dependence of the speed of detection of the KF on the starting angle of the disturbances is also addressed. One drawback is that the KF has some regions of slowness.

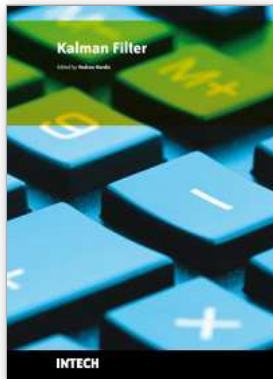
To overcome this, a fast detection method for sags, swells, and interruptions based on the combination of the KF and the digital RMS algorithm can be used. When combined, the advantage of high speed of the KF at some regions is availed, and the slowness it has at other regions is rejected with the digital RMS method. The KF-RMS algorithm considers the dependence of the time of detection on all possible electrical angles at which a disturbance could appear, sag depths from $0.1p.u.$ to the complete interruption, swell rises from $1.1p.u.$ to $2.0p.u.$, and an amount of harmonics that is higher than the allowed by the most important worldwide standards on voltage harmonic levels in practical electrical systems, leaving apart in this way the ideal and non practical case. The method has a very high probability that all events are detected in less than a quarter of cycle, and more than 50% of probability they are detected in less than $2ms$, which can be considered very fast. A small zone of angles and depths at which the method takes more than a quarter of cycle to detect disturbances exists, but indeed, detection times will never be equal or greater than half cycle. The performance of the KF-RMS method is also affected by the sampling frequency. However, this dependence can be eliminated by selecting an adequate Q matrix for each sampling frequency. Experimental tests of the method validate and strengthen the contribution in detection of disturbances.

The application of the KF as estimator of parameters for power quality monitoring is also addressed. It can be applied for the estimation of the magnitude, frequency, and phase of the fundamental and harmonic components of a signal, in an independent way, or simultaneously using any combination of them. The collected information can be recorded and used to obtain statistics on the behavior of a voltage or current within a lapse of time, such as the steady state parameters and the number voltage variations, with their classification and characterization. This monitoring information can be used to propose solutions for power quality improvement. The correct definition of the model is crucial to have the desired estimations. An actual fact is that the KF proves to be a very useful and advantageous algorithm to help improving power quality in a variety of ways.

7. References

- Affolter, R. & Connell, B. (2003). Experience with a dynamic voltage restorer for a critical manufacturing facility, *Proceedings of the IEEE PES Transmission and Distribution Conference and Exposition*, Vol. 3, pp. 937 – 939, ISBN 0-7803-8110-6, Sept. 2003.
- Baitch A. & Barr R.A. (1985). A tapping range and voltage level analysis chart for tap changing transformers, *IEEE Transactions on Power Apparatus and Systems*, Vol. PAS-104, Issue 11, Nov 1985, pp. 3269-3277, ISSN 0018-9510.
- Bhadkamkar A.; Bendre A.; Schneider R.; Kranz W. & Divan D. (2003). Application of zig-zag transformers in a three-wire three-phase dynamic sag corrector system, *Proceedings of the 34th Annual IEEE Power Electronics Specialist Conference 2003 PESC 03*, Vol. 3, pp. 1260-1265, 15-19, ISBN 0-7803-7754-0, June 2003.
- Bollen M.H.J. (2000). *Understanding Power Quality Problems: Voltage Sags and Interruptions*, IEEE Press, ISBN 0-7803-4713-7, New York, USA.
- Dash, P.K.; Sahoo, D.K.; Panigrahi, B.K. & Panda, G. (2001). Integrated spline wavelet and Kalman filtering approach for power quality monitoring in a power network, *Proceedings of the 4th IEEE International Conference on Power Electronics and Drive Systems*, Vol. 2, pp. 858-863, ISBN 0-7803-7233-6, Oct. 2001.
- Deckmann, S.M. & Ferreira, A.A. (2002). About voltage sags and swells analysis, *Proceedings of the 10th International Conference on Harmonics and Quality of Power*, Vol. 1, pp. 144-148, ISBN 0-7803-7671-4, Oct. 2002.
- Dugan R.C.; McGranaghan M.F.; Santoso S. & Beaty H.W. (2003). *Electrical Power Systems Quality*, McGraw Hill, ISBN 0-07-138622-X, USA.
- Fitzer C.; Barnes M. & Green P. (2004). Voltage sag detection technique for a dynamic voltage restorer, *IEEE Transactions on Industry Applications*, Vol. 40, Issue 1, Jan-Feb 2004, pp. 203-212, ISSN 0093-9994.
- Fletcher D.L. & Stadlin W.O. (1983). Transformer tap position estimation, *IEEE Transactions on Power Apparatus and Systems*, Vol. PAS-102, Issue 11, Nov 1983, pp. 3680-3686, ISSN 0018-9510.
- Girgis A.A.; Chang W.B. & Makram E.B. (1991). A digital recursive measurement scheme for on-line tracking of power system harmonics, *IEEE Transactions on Power Delivery*, Vol. 6, No. 3, July 1991, pp. 1153-1160, ISSN 0885-8977.
- González M.; Cárdenas V. & Álvarez R. (2006). Detection of sags, swells and interruptions using the digital RMS method and Kalman filter with fast response, *Proceedings of the 32nd Annual Conference of the IEEE Industrial Electronics Society IECON2006*, pp. 2249-2254, ISBN 1-4244-0391-X, Paris, France, November 2006.
- González M.; Cárdenas V. & Álvarez R. (2008). A fast detection algorithm for sags, swells, and interruptions based on digital RMS calculation and Kalman filtering, *Submitted to IEEE Transactions on Aerospace and Electronic Systems*.

- Hingorani N.G. & Gyugyi L. (2000). *Understanding FACTS: Concepts and Technology of Flexible AC Transmission Systems*, IEEE Press, ISBN 0-7803-3455-8, New York, USA.
- IEEE Std 519-1992 (1993). *IEEE Recommended Practices and Requirements for harmonic Control in Electrical Power Systems*, IEEE inc., ISBN 1-55937-239-7, New York, USA.
- IEEE Std 1100-2005 (2006). *IEEE Emerald Book, Recommended Practice for Powering and Grounding Electronic Equipment*, IEEE inc., ISBN 0-7381-4979-9, New York, USA.
- IEEE Std 1159-1995 (1995). *IEEE Recommended Practice for Monitoring Electric Power Quality*, IEEE inc., ISBN 1-55937-549-3, New York, USA.
- IEEE Std 1159.3-2003 (2004). *IEEE Recommended Practice for the Transfer of Power Quality Data*, IEEE inc., ISBN 0-7381-3578-X, New York, USA.
- Joos, G.; Su Chen & Lopes, L. (2004). Closed-loop state variable control of dynamic voltage restorers with fast compensation characteristics, *Proceedings of the IEEE 39th IAS Annual Meeting Industry Applications Conference*, Vol. 4, pp. 2252 - 2258, ISBN 0-7803-8486-5, Oct. 2004.
- Ma H. & Girgis A.A. (1996). Identification and tracking of harmonic sources in a power system using Kalman filter, *IEEE Transactions on Power Delivery*, Vol. 11, No. 3, July 1996, pp. 1659-1665, ISSN 0885-8977.
- Martínez G. S. (1992). *Alimentación de equipos informáticos y otras cargas críticas (In Spanish)*, Mc-Graw-Hill, ISBN 84-7615-920-X, Spain.
- Montero-Hernández O.C. & Enjeti P.N. (2005). A fast detection algorithm suitable for mitigation of numerous power quality disturbances, *IEEE Transactions on Industry Applications*, vol. 41, Issue 6, Nov.-Dec. 2005, pp. 2661-2666, ISSN 0093-9994.
- Nielsen J.G.; Newman M.; Nielsen H. & Blaabjerg, F. (2004). Control and testing of a dynamic voltage restorer (DVR) at medium voltage level, *IEEE Transactions on Power Electronics*, Vol. 19, Issue 3, May 2004, pp. 806 - 813, ISSN 0885-8993.
- Saleh S.A. & Rahman M.A. (2004). Wavelet-based dynamic voltage restorer for power quality improvement, *Proceedings of the IEEE 35th Annual Power Electronics Specialists Conference PESC04*, Vol. 4, pp. 3152-3156, ISBN 0-7803-8399-0, June 2004.
- Sannino A.; Miller M.G. & Bollen M.H.J. (2000). Overview of Voltage Sag Mitigation, *Proceedings of the IEEE Power Engineering Society Winter Meeting*, Vol. 4, pp. 2872-2878, ISBN 0-7803-5935-6, January 2000.
- Schwartzberg, J.W.; Nwankpa, C.O.; Fischl, R. & Sundaram, A. (1994). Prediction of distribution system disturbances, *Proceedings of the IEEE 25th Annual Power Electronics Specialists Conference PESC94*, Vol. 2, pp. 1077-1082, ISBN 0-7803-1859-5, June 1994.
- Vilathgamuwa D.M., Perera A.A.D. & Choi S.S. (2003). Voltage sag compensation with energy optimized dynamic voltage restorer, *IEEE Transactions on Power Delivery*, Vol. 18, July 2003, pp. 928 - 936, ISSN 0885-8977.
- Wang K., Zhuo F., Li Y., Yang X. & Wang Z. (2004). Three-phase four-wire dynamic voltage restorer based on a new SVPWM algorithm, *Proceedings of the IEEE 35th Annual Power Electronics Specialists Conference PESC 04*, Vol. 5, pp. 3877 - 3882, ISBN 0-7803-8399-0, June 2004.
- Wunderlin, T.; Amhof, O.; Dahler, P. & Guning, H. (1998). Power supply quality improvement with a dynamic voltage restorer (DVR), *Proceedings of the International Conference on Energy Management and Power Delivery EMPD98*, Vol. 2, pp. 518 - 525, ISBN 0-7803-4495-2, March 1998.
- Yu K.K.C.; Watson N.R. & Arrillaga J. (2005). An adaptive Kalman filter for dynamic harmonic state estimation and harmonic injection tracking, *IEEE Transactions on Power Delivery*, Vol. 20, No. 2, April 2005, pp. 1577-1584, ISSN 0885-8977.
- Zamora B. M. & Macho S. V. (1997). *Distorsión armónica producida por convertidores estáticos (In Spanish)*, Iberdrola, ISBN 84-921269-1-9, Spain.



Kalman Filter

Edited by Vedran Kordic

ISBN 978-953-307-094-0

Hard cover, 390 pages

Publisher InTech

Published online 01, May, 2010

Published in print edition May, 2010

The Kalman filter has been successfully employed in diverse areas of study over the last 50 years and the chapters in this book review its recent applications. The editors hope the selected works will be useful to readers, contributing to future developments and improvements of this filtering technique. The aim of this book is to provide an overview of recent developments in Kalman filter theory and their applications in engineering and science. The book is divided into 20 chapters corresponding to recent advances in the field.

How to reference

In order to correctly reference this scholarly work, feel free to copy and paste the following:

Mario Gonzalez and Victor Cardenas (2010). The Kalman Filter in Power Quality – Theory and Applications, Kalman Filter, Vedran Kordic (Ed.), ISBN: 978-953-307-094-0, InTech, Available from:
<http://www.intechopen.com/books/kalman-filter/the-kalman-filter-in-power-quality-theory-and-applications>

INTECH
open science | open minds

InTech Europe

University Campus STeP Ri
Slavka Krautzeka 83/A
51000 Rijeka, Croatia
Phone: +385 (51) 770 447
Fax: +385 (51) 686 166
www.intechopen.com

InTech China

Unit 405, Office Block, Hotel Equatorial Shanghai
No.65, Yan An Road (West), Shanghai, 200040, China
中国上海市延安西路65号上海国际贵都大饭店办公楼405单元
Phone: +86-21-62489820
Fax: +86-21-62489821

© 2010 The Author(s). Licensee IntechOpen. This chapter is distributed under the terms of the [Creative Commons Attribution-NonCommercial-ShareAlike-3.0 License](#), which permits use, distribution and reproduction for non-commercial purposes, provided the original is properly cited and derivative works building on this content are distributed under the same license.